First palaeohistological inference of resting metabolic rate in an extinct synapsid, Moghreberia nmachouensis (Therapsida: Anomodontia)

Chloe Olivier, Alexandra Houssaye, Nour-Eddine Jalil, Jorge Cubo

First palaeohistological inference of resting metabolic rate in extinct synapsid, Moghreberia nmachouensis (Therapsida: Anomodontia)

CHLOE OLIVIER[1,2], ALEXANDRA HOUSSAYE[3], NOUR-EDDINE JALIL[2] and JORGE CUBO[1*]

[1] Sorbonne Universités, UPMC Univ Paris 06, CNRS, UMR 7193, Institut des Sciences de la Terre Paris (iSTeP), 4 place Jussieu, BC 19, 75005, Paris, France

[2] Sorbonne Universités -CR2P -MNHN, CNRS, UPMC-Paris6. Muséum national d'Histoire naturelle. 57 rue Cuvier, CP38. F-75005, Paris, France

[3]Département Écologie et Gestion de la Biodiversité, UMR 7179, CNRS/Muséum national d'Histoire naturelle, 57 rue Cuvier, CP 55, Paris, 75005, France

*Corresponding author. E-mail: jorge.cubo_garcia@upmc.fr

Running title: Bone histology of *Moghreberia nmachouensis*

ABSTRACT

The independent acquisitions of endothermy in synapsids and diapsids are major events in vertebrate evolution since they were the driving force of a suite of correlated changes in anatomical, physiological, behavioral and ecological traits. While avian endothermy is assumed to have occurred at the archosauriform node, the acquisition of mammalian endothermy is poorly constrained both temporally and phylogenetically. Among the many unequivocal anatomical correlates of endothermy in synapsids, the presence of insulative pelage or respiratory turbinates only allows discrete inferences of presence / absence of endothermy. The analysis of bone histology allows richer paleobiological inferences. We described the osteohistology and growth patterns of *Moghreberia nmachouensis* and two related taxa (*Lystrosaurus* and *Oudenodon*) for comparative purposes. Our observations suggest increasing growth rates from *Moghreberia* (presence of incipient fibro-lamellar bone, FLB, in humerus and femur), to *Lystrosaurus* (presence of well developed FLB in the femur but presence of incipient FLB in the humerus), to *Oudenodon* (presence of well developed FLB in humerus and femur). However, qualitative histology does not allow reliable inferences about the occurrence of endothermy. We performed the first quantitative inferences of resting metabolic rates on fossil synapsids (*Moghreberia nmachouensis* as a model and *Lystrosaurus* and *Oudenodon* for comparative purposes) using quantitative histology (osteocyte lacunae size, shape and density) combined with phylogenetic eigenvector maps. Our inferences are consistent with our qualitative histological observations: the mass-independent resting metabolic rate inferred for *Moghreberia nmachouensis* (2.58 $mLO_2\ h^{-1}\ g^{-0.67}$) is lower than the value inferred for *Lystrosaurus* (3.80 $mLO_2\ h^{-1}\ g^{-0.67}$), which is lower than that inferred for *Oudenodon* (4.58 $mLO_2\ h^{-1}\ g^{-0.67}$). Optimization of these inferences onto

a phylogenetic tree of amniotes using the parsimony method allowed us to better constrain the temporal (more than 260 My ago) and phylogenetic (Neotherapsida) frames of the acquisition of mammalian endothermy.

KEYWORDS : Dicynodontia – Endothermy – Fibrolamellar bone - Paleohistology - Phylogenetic eigenvector maps

INTRODUCTION

The acquisition of mammalian endothermy is a major event in vertebrate evolution since it modified the energetic relationships between organisms and their environment (Walter and Seebacher, 2009). To constrain the temporal and phylogenetic frames of this event, we need to identify unequivocal anatomical correlates of endothermy (Ruben *et al*., 2012). Among them, the oldest evidence for an insulative pelage (through fossilized fur impressions) has been found in the Middle Jurassic non-mammalian therapsids (*Castorocauda*, Ji *et al.*, 2006; *Megaconus,* Zhou *et al.,* 2013*; Agilodocodon,* Meng *et al.,* 2015), but it seems that the acquisition of endothermy based on increased aerobic capacity is older (Ruben *et al.*, 2012). The presence of respiratory turbinates is another anatomical feature linked to endothermy. Although these structures are rarely preserved in fossils, bone ridges of turbinate attachment are frequently preserved (Ruben *et al.*, 2012). These structures are first recognizable in therocephalians and in cynodonts (Ruben *et al.*, 2012), so they may have been acquired by the eutheriodonts. Thermic modeling (Florides *et al.*, 2001) and the isotopic composition of mineralized remains (Rey, 2016) have also been used to infer the physiological thermoregulation of non-mammalian synapsids.

Bone paleohistology is a useful method to infer the bone growth rates and resting metabolic rates of extinct vertebrates. The bone histology of non-mammalian synapsids has been intensively studied in the last decade. Laurin & Buffrénil (2016) analyzed the ophiacodont *Clepsydrops collettii* and concluded that the femur is made of woven-fibered tissue combined with parallel-fibered bone in primary osteons. Shelton and Sander (2015) reported the presence of fibrolamellar bone (FLB) in *Ophiacodon retroversus*, *O. uniformis* and *O. mirus*. Shelton *et al*. (2013) reported “incipient fibrolamellar bone” in

the humerus and femur of *Dimetrodon natalis.* Botha-Brink and Angielczyk (2010) analyzed a sample of Anomodontia and showed the presence of FLB in the dromasaur *Galeops* and the dicynodonts *Eodicynodon, Diictodon*, *Endothiodon, Cistecephalus, Dicynodontoides, Rhachiocephalus, Aulacephalodon, Tropidostoma, Oudenodon, Dicynodon, Kannemeyeria, Lystrosaurus declivis*, *L. murrayi* and *L. maccaigi*. Ray, Chinsamy & Bandyopadhyay (2005) analyzed also the bone histology of *L. murrayi* and showed the presence of FLB in the humerus, femur, tibia and a proximal phalanx. Chinsamy & Ray (2012) reported FLB tissue in the long bones of two Gorgonopsia (*Scylacops* and *Aelurognathus*) and in the tibia and fibula of two undertermined Therocephalia. Huttenlocker and Botha-Brink (2014) concluded that basal therocephalians (e.g., *Lycosuchus*) are characterized by highly vascularized FLB whereas Eutherocephalia (but *Moschorhinus*) lack this condition (e.g., *Theriognathus*). Some authors analyzed the histological features of non-mammalian cynodonts and showed the presence of FLB in *Procynosuchus, Trucidocynodon* and *Langbergia* (Botha-Brink, Abdala & Chinsamy, 2012)*, Thrinaxodon* (Botha and Chinsamy, 2005; Botha-Brink et al., 2012; de Ricqlès, 1969)*, Cynognathus* and *Diademodon* (Botha and Chinsamy, 2000; Botha-Brink et al., 2012)*, Trirachodon* (Botha and Chinsamy, 2004; Botha-Brink et al., 2012)*,,* and *Tritylodon* (Botha-Brink et al., 2012; Chinsamy and Hurum, 2006; de Ricqlès, 1969; Ray, Botha & Chinsamy, 2004). All these studies were carried out using classic qualitative histology. Results obtained using this approach are useful to infer bone growth rates assuming Amprino's rule (e.g., Montes, Castanet & Cubo, 2010), i.e., considering that the organization of the collagenous wave and of the vascular network in the osseous tissue are strongly correlated with bone growth rate. However, they are not suitable to infer resting metabolic rates or physiological thermoregulation. Indeed, it has been shown that some extant ectotherms (e.g., the alligators) are able to form lamellar-

zonal bone (de Ricqlès, Padian & Horner, 2003; Lee, 2004) but also FLB both in captivity (Padian, Horner & de Ricqlès, 2004) and in the wild (Tumarkin-Deratzian, 2007), probably an atavistic characteristic of an endothermic ancestry among archosaurs (Seymour et al. 2004).

Recent developments in quantitative bone histology have facilitated the first direct inferences of resting metabolic rates in extinct diapsids (Legendre *et al.*, 2016). This study is aimed at performing the first quantitative inferences of resting metabolic rates on fossil synapsids, using three dicynodonts as models (*Moghreberia nmachouensis* *Lystrosaurus* and *Oudenodon*). Dicynodonts are among the most abundant terrestrial herbivores from the middle Permian to late Triassic. They were cosmopolitan and had a wide range of ecologies and morphologies represented by an abundant and diversified fossil record. *Myosaurus* and the rich-species genus *Lystrosaurus* survived the P/T crisis (Maisch and Matzke, 2014). Therefore, dicynodonts are good models to gain a better understanding of the impact of this biotic crisis on terrestrial ecosystems. This survey is focused on the Moroccan Upper Triassic *Moghreberia nmachouensis* but includes the Permian *Oudenodon bainii* and Lystrosaurus for comparative purposes. Only the cranial material of the monospecific genus *Moghreberia* was shortly described by Dutuit (1988). *Moghreberia* is a kannemeyeriiform, the most frequent group in Triassic, but its phylogenetic position is discussed. Certain authors considered it as a synonym of the Upper Triassic North-American dicynodont *Placerias* (Cox, 1991) while others supposed they are sister-groups (Kammerer, Fröbisch & Angielczyk, 2013). In addition to inferring the resting metabolic rates of *Moghreberia nmachouensis*, we will describe the osteohistology and growth patterns of this taxon, using two related taxa (*Lystrosaurus* and *Oudenodon*) for comparative purposes.

MATERIAL AND METHODS

MATERIAL

The material consists of humeral and femoral mid-diaphyseal transverse sections of the Moroccan Upper Triassic *Moghreberia nmachouensis* (femur MNHN.F.ALM 100 of 310 mm in length, and humerus MNHN.F.ALM 297 of 375 mm in length; Fig. 1) and of two additional dicynodonts from the personal collection of Armand de Ricqlès (research collection, Museum National d'Histoire Naturelle, Paris, France). On the one hand, *Lystrosaurus* sp. (humerus 24.1 of 131 mm in length, and femur 11-15 of 90.7 mm in length without the proximal epiphysis) from the Triassic *Lytrosaurus* assemblage zone of the South African Karoo Basin (de Ricqlès, 1969), where *Lystrosaurus curvatus*, *L. declivis* and *L. murrayi* have been discovered (Botha & Smith, 2007; Fröbisch, 2009; de Ricqlès, 1972; Smith and Botha, 2005). On the other hand *Oudenodon baini* (humerus 292-1 of 119 mm in length, and an unnumbered femur of 107 mm in length) from the *Cynognathus* assemblage zone of the South African Karoo Basin (de Ricqlès, 1969). Humerus and femur came from different specimens in all three taxa.

HISTOLOGY

Bones were molded prior to sectioning. All sections were made at the mid-diaphysis using standard procedures (e.g., Padian & Lamm, 2013; only the central part of the diaphyses have been embedded in a polyester resin). Sections were observed microscopically using Leica DM2700 P and Zeiss Axiovert 35 (Jena, Germany) microscopes under natural and polarized light and photographed using a DXM 1200

Digital Eclipse Camera System (Nikon, Japan) and an Olympus Digital Camera (Japan). Sections were also scanned using a high-resolution Epson V740 PRO scanner. The histological terminology follows Francillon-Vieillot *et al.* (1990).

INFERENCE MODELS

We constructed two resting metabolic rate inference models (for the humerus and for the femur) using phylogenetic eigenvector maps, a new powerful approach developed by Guenard, Legendre & Peres-Neto (2013) and recently used by Legendre *et al.* (2016). The interest of this approach lies in the fact that it takes into account both phylogenetic and phenotypic information (here bone quantitative histology) to perform paleobiological inferences. We used a sample of seventeen extant amniotes (*Pleurodeles waltl, Microcebus murinus, Lepus europaeus, Oryctolagus cuniculus, Cavia porcellus, Mus musculus, Capreolus capreolus, Zootoca vivipara, Podarcis muralis, Varanus exanthematicus, Varanus niloticus, Chelodina oblonga, Pelodiscus sinensis, Trachemys scripta, Crocodylus niloticus, Gallus gallus* and *Anas platyrhynchos*) for which we know both the variable to be inferred in extinct taxa (resting metabolic rate), and the quantified histological features (size, shape, and density of osteocyte lacunae in primary bone outside osteons). The bone histological data (size, shape, and density of osteocyte lacunae in primary bone outside osteons) for all extant taxa but *Lepus europaeus, Oryctolagus cuniculus* and *Capreolus capreolus* were taken from Legendre *et al.* (2016). Bone histological data for the quoted three taxa were quantified in this study. Mass-independent resting metabolic rate (in $mLO_2\ h^{-1}\ g^{-0.67}$) for all extant taxa but *Lepus,*

Oryctolagus and *Capreolus* were experimentally quantified by Montes *et al.* (2007). Mass-independent resting metabolic rate for the quoted three taxa were taken respectively from Hackländer, Arnold & Ruf (2002), Seltmann, Ruf & Rödel (2009) and Mauget, Mauget and Sempéré (1999). We quantified the quoted bone histological variables in the humeri and femora of the taxa for which we aim to infer the resting metabolic rate (*Moghreberia nmachouensis*, *Lystrosaurus* and *Oudenodon*) using the procedure described by Legendre *et al*. (2016). Osteohistological data of extant growing tetrapods species taken from Legendre *et al.* (2016) were quantified in the outer cortex, whereas osteohistological measurements performed in this study for three adult extant mammals (*Lepus europaeus, Oryctolagus cuniculus* and *Capreolus capreolus*) and three sub-adult or adult extinct synapsids (*Moghreberia nmachouensis*, *Lystrosaurus* and *Oudenodon*) were made in the deep cortex. In addition to this histological information, the structure of a phylogenetic tree was taken into account, expressed as a set of eigenfunctions, termed phylogenetic eigenvector maps. Afterwards, a subset of phylogenetic eigenfunctions and bone histological variables were selected to infer resting metabolic rates for species in the tree for which these trait data are otherwise lacking (*Moghreberia nmachouensis*, *Lystrosaurus* and *Oudenodon*). For each model (one constructed using femora and another using humeri), we calculated the AIC values (Akaike information criterion) to select the osteohistological variable (osteocyte lacunae density, size or shape) best fits with the phylogeny transcribed as eigenvectors. We choose the variable corresponding to the smallest AIC value. The combination of this selected variable and the eigenvectors (i.e. the phylogeny) allowed us to predict the dependent variable (metabolic rate) unknown in fossils. We performed the analyses using the R package MPSEM (Guénard *et al.*, 2013) and constructed an inference model for each bone (humerus and femur). We selected the best set of variables among

phylogenetic eigenvector maps plus one of the three histological characters, using their Akaike information criterion corrected for finite sample sizes (Burnham, Anderson & Huyvaert, 2011), and cross-validated using leave-one-out cross-validation. Indeed, including more than one histological co-predictor might have been a potential source of power loss considering our rather small sample size (Legendre et al., 2016). In this way we were able to infer the resting metabolic rates of *Moghreberia nmachouensis*, *Lystrosaurus* and *Oudenodon* with their 95% confidence intervals. We obtained two resting metabolic rate values for each taxon, one using the humerus and the other using the femur. We used the highest estimation in our comparative analysis because a given specimen with the resting metabolic rate of an endotherm (e.g., *Microcebus murinus*, Montes *et al.,* 2007) can grow slowly (*M. murinus,* Castanet *et al.,* 2004) but the contrary is not true (e.g., ectotherms including active animals such as *Varanus* have low resting metabolic rates and grow slowly; Montes *et al.,* 2007).

RESULTS

MICROANATOMICAL FEATURES

The humerus microstructure is relatively homogeneous with thin osseous trabeculae and reduced intertrabecular spaces occupying most of the section (Fig. 1A). The medullary area is difficult to distinguish from the cortex, although the tightness of the spongiosa becomes tighter (smaller intertrabecular spaces) away from the section center.

The femur displays a thick compact cortex with a distinct medullary zone occupied by thin osseous trabeculae (Fig. 1B). Unfortunately the state of preservation

prevents us to conclude if an open medullary cavity occurred in the core of the section or if the whole medullary area was occupied by a spongiosa.

HISTOLOGICAL FEATURES

Moghreberia nmachouensis humerus. Bone is highly vascularized. An intense remodelling (i.e., process of bone resorption and the subsequent deposition of new bone over the resorption surfaces) extends from the inner to the outer cortex. It is of two types: 1) centripetal secondary bone platings on resorption lines (numerous cementing lines in various directions) with no formation of secondary osteons (Fig. 2A), on most of the section; and 2) Haversian remodelling, with secondary osteons (Fig. 2B), on the posterior and dorsal borders. Remains of primary bone are rare. They nevertheless suggest that primary bone consists in incipient fibrolamellar bone (sensu Klein [2010]; Fig. 2C), i.e., with primary bone consisting of both parallel-fibered and woven bone and the vascular canals not being all primary osteons. Avascular parallel-fibered bone (PFB) is observed at the periphery of the outer cortex locally along the posteroventral and posterodorsal borders. It is also observed as thin layers alternating with layers of incipient fibrolamellar bone (iFLB), illustrating an alternation of zones (iFLB) and annuli (PFB; Fig. 2C). Important concentrations of Sharpey's fibers inserted rather perpendicularly to the collagen fibers are observed at the three pointed extremities of the section.

Moghreberia nmachouensis femur. As opposed to what is observed in the humerus, the femur is essentially composed of Haversian bone and remodelling extends up to the periphery of the outer cortex on the posteromedial and anterolateral borders, with only a few remains of primary bone on the periphery. The transition zone between

the cortex and the medullary area is characterized by a loose spongiosa of secondary bone with only a few secondary osteons that show a large lumen (Fig. 2D). Bone vascularity is high in most of the cortex but the vascular canal density decreases in the periphery of the anteromedial and anterolateral borders. Primary bone also consists of incipient FLB with some osteons aligned in concentric layers, alternating with thin layers of avascular parallel-fibered bone. Vascular canals are essentially longitudinal with circular and radial (even oblique) anastomoses. Sharpey's fibers are concentrated on the posterior border (less on the anterolateral and anteromedial borders). On the posteromedial border, they are associated with a modification of the vascular canal orientation, the latter being oriented in the same direction as the fibers).

Neither the humerus nor the femur of *Moghreberia nmachouensis* show a high concentration of growth marks or even a layer of parallel-fibered bone (thicker than an annulus) near the bone periphery.

Lystrosaurus and *Oudenodon* humeri and femora were analyzed for comparative purposes. *Lystrosaurus* humerus shows incipient FLB (Fig. 3A) whereas *Lystrosaurus* femur shows well developed FLB (Fig. 3B). *Oudenodon* femur (Fig. 3C) and humerus (not shown) are composed of well developed FLB. *Lystrosaurus* and *Oudenodon* humeri and femora show a lower quantity of secondary bone than the corresponding *Moghreberia* bones.

RESTING METABOLIC RATE INFERENCE MODELS

For the humerus, the Akaike information criterion (AIC) suggests that the more accurate model includes the shape of osteocyte lacunae in addition to the selected phylogenetic eigenvector maps (R-squared = 0.9901686; AIC score = 18.66448). The mass-

independent resting metabolic rate values (in $mLO_2\ h^{-1}\ g^{-0.67}$) inferred for the three taxa are: *Moghreberia*: 1.76 (95% confidence interval or $CI_{95\%}$=[1.31; 2.37]); *Lystrosaurus*: 2.43 ($CI_{95\%}$=[1.95; 3.03]); *Oudenodon*: 1.09 ($CI_{95\%}$=[0.88; 1.34]).

For the femur, the AIC suggests a model that includes the osteocyte lacunae density in addition to the selected phylogenetic eigenvector maps (R-squared = 0.993772; AIC score = 18.61558). The resting metabolic rate values (in $mLO_2\ h^{-1}\ g^{-0.67}$) inferred for the three taxa are: *Moghreberia*: 2.58 ($CI_{95\%}$=[1.94; 3.43]); *Lystrosaurus*: 3.80 ($CI_{95\%}$=[3.04; 4.76]); *Oudenodon*: 4.58 ($CI_{95\%}$=[3.63; 5.82]).

As stated in the methods section, of the two mass-independent resting metabolic rate values inferred for each taxon (one using the model constructed using femora and the other using the model constructed using humeri), we used the higher one in our comparative analysis. In all three taxa the higher value was inferred using the femora. These values are represented in figure 4 together with values experimentally measured in extant taxa.

DISCUSSION

The parsimony method suggests that avian and mammalian endothermies are convergent (i.e., non-inherited from a common ancestor). These independent acquisitions of endothermy are major events in vertebrate evolution since they were the driving force of a suite of correlated changes in the respiratory and the circulatory systems, as well as in physiological, behavioral and ecological traits (Seymour *et al*., 2004).

Bone paleohistology is a reliable method that has been extensively used to infer the resting metabolic rates and physiological thermoregulation of extinct diapsids. Two

approaches have been used. On the one hand, several authors performed *indirect* inferences of physiological thermoregulation assuming a relationship between bone growth rates and resting metabolic rate (Montes *et al*., 2007). Indeed, Ricqlès *et al.* (2003, 2008) inferred bone growth rates from bone tissue types using a qualitative approach and Amprino's rule (Montes *et al.*, 2010). Other authors performed quantitative paleohistological inferences of bone growth rates (Cubo *et al.*, 2012; Legendre, Segalen & Cubo, 2013). On the other hand, some authors performed *direct* inferences of resting metabolic rates in extinct diapsids using bone paleohistology and phylogenetic eigenvector maps (Legendre *et al.*, 2016). Here we used qualitative and quantitative histology to infer respectively growth patterns and resting metabolic rates of *Moghreberia nmachouensis*.

GROWTH RATE AND STAGE

(1) Ontogenetic stage. The *Moghreberia* humeral section shows a high remodelling activity and, in periphery, a cyclical growth with zones and annuli. Following the analysis of Ray *et al.* (2005) on *Lystrosaurus*, this would suggest, if *Moghreberia* grows in a similar way as *Lystrosaurus*, that the individual was at least sub-adult. Similarly, high remodelling has been tentatively interpreted as suggesting a non-juvenile ontogenetic stage (Ray & Chinsamy, 2004; Ray *et al.*, 2004). This is consistent with the anatomy that suggests an sub-adult ontogenetic stage.

The femoral section shows again a high remodelling activity, and an alternation of zones and annuli associated with a reduction in the degree of vascularization towards the bone periphery. Although the morphology suggests a juvenile ontogenetic stage (small size, loss of the epiphyses; Gale [1988]), the histology is rather in accordance with

an at least sub-adult ontogenetic stage (Ray *et al.*, 2005, Ray, Bandyopadhyay & Appana, 2010).

(2) Growth rate. The occurrence of well developed FLB and the very high vascularization observed in *Lystrosaurus* femur (Fig. 3B) and *Oudenodon* femur (Fig. 3C) and humerus (not shown) evoke previous observations made on the Permian dicynodonts *Endothiodon*, *Diictodon*, *Oudenodon* and *Tropidostoma* (Chinsamy & Rubidge, 1993; Botha, 2003;Botha & Angielczyck, 2007, 2010) and theTriassic dicynodonts *Placerias*, *Lystrosaurus*, *Wadiasaurus* and *Kannemeyeria* (Botha-Brink & Angielczyck, 2010; Green, Schweitzer & Lamm, 2010; Ray *et al.,* 2005, 2010, Ray, Botha & Chinsamy, 2012; Green & Chinsamy-Turan, 2012). In contrast, *Moghreberia* humerus and femur and *Lystrosaurus* humerus lack a well developed FLB but show incipient FLB. Fibrolamellar bone is generally observed in mammals and birds (e.g., Chinsamy & Elzanowski 2001; Kolb *et al.*, 2015) and associated with rapid osteogenesis in extant and extinct taxa (e.g., Chinsamy & Rubidge, 1993; Padian, de Ricqlès & Horner, 2001; Ray & Chinsamy, 2004; Chinsamy & Tumarkin-Deratzian, 2009). As bone growth rate is associated, though indirectly, to metabolic rate (Reid, 1987; Padian *et al.*, 2001; Chinsamy-Turan, 2005; Montes *et al.*, 2007), FLB is generally associated with endothermy. Please keep in mind that although FLB is also observed in some ectothermic Crocodylia (Tumarkin-Deratzian, 2007; Woodward Ballard, Horner & Farlow, 2014), this presence is probably an atavistic characteristic inherited from the endothermic last common ancestor of archosaurs (Seymour et al. 2004).

Incipient FLB, described by Klein (2010), has also been observed in temnospondyls (Konietzko-Meier & Schmitt, 2013), sauropterygians (pachypleurosaurs, nothosaurs; Klein, 2012; Klein et al., 2016), phytosaurs (Ricqlès *et al.*, 2003), mosasaurs (Houssaye *et al.*, 2013), but also in the pelycosaur *Dimetrodon* (Shelton *et al.*, 2013).

Considering that it has been shown that the parallel-fibered bone is formed at a lower growth rate than the woven bone, the presence of incipient FLB suggest a lower growth rate than the presence of well developed FLB. Therefore, qualitative histological observations suggest increasing growth rates from *Moghreberia* (presence of incipient FLB in humerus and femur) to *Oudenodon* (presence of well developed FLB in humerus and femur), and intermediate values for *Lystrosaurus* (presence of well developed FLB in the femur but presence of incipient FLB in the humerus). However, qualitative histology does not allow reliable inferences about the occurrence of endothermy.

(3) Bone remodelling. The strong remodelling in the long bones of *Moghreberia* evokes that observed in *Placerias* and *Kannemeyeria* (Green *et al.*, 2010; Ray *et al.*, 2012). It is, however, much more limited in other dicynodonts, where it essentially occurs in the medullary spongiosa and only extends up to the perimedullary region in adult specimens (Ray & Chinsamy, 2004; Ray *et al.*, 2005, 2009, 2012; Botha-Brink & Angielczyck, 2010), and where it is much scarcer in the rest of the cortex. Bone remodelling is interpreted as reflecting biomechanical constraints (Currey, 2003; Skedros *et al.*, 2007), but is also considered associated with an active metabolism (Currey, 2003), related to the blood flow of the bone vascular network (Seymour *et al.,* 2012), or to the size of the skeletal elements (Padian, Werning & Horner, 2016). This would be consistent with the hypothesis of a high metabolism in *Moghreberia*. However, comparative data remain too limited to discuss further the possible physiological significance of bone remodelling.

RESTING METABOLIC RATE INFERENCE MODELS

Paleobiological inferences obtained using femoral quantitative histology (osteocyte lacunae size, shape and density) and phylogenetic eigenvector maps suggest that the three taxa analysed - *Moghreberia nmachouensis, Lystrosaurus* and *Oudenodon baini* - had high mass-independent resting metabolic rates ($mLO_2\ h^{-1}\ g^{-0.67}$), similar to, or even higher than those observed in some of the extant mammals from our sample (Fig. 4). These inferences are congruent with the conclusions obtained using qualitative histology (see above), according to which, assuming Amprino's rule, bone growth rates may increase from *Moghreberia* (characterized by the presence of incipient FLB in humerus and femur), to *Lystrosaurus* (presence of incipient FLB in the humerus but presence of well developed FLB in the femur) to *Oudenodon* (presence of well developed FLB in both the humerus and the femur). Of the two mass-independent resting metabolic rate values inferred for each taxon (one using the femur and other using the humerus), we used the higher one (that obtained using the femur; cf. methods) in our comparative analysis. Of the three extinct taxa analyzed, *Oudenodon* had the highest mass-independent resting metabolic rate. This result is the outcome of two facts (1) the histological variable selected by the phylogenetic eigenvector maps for the femoral model was osteocyte lacunae density, and (2) *Oudenodon* shows the highest osteocyte lacunae density (0.00496 osteocyte lacunae / μm^2), followed by *Lystrosaurus* (0.00428 osteocyte lacunae / μm^2) and *Moghreberia* (0.00316 osteocyte lacunae / μm^2). Thus paleobiological inferences performed in this study are robust because results obtained using quantitative histology and phylogenetic eigenvector maps are consistent with those obtained using qualitative histology.

Rey (2016) analyzed the isotopic composition of mineralized tissues and concluded that endothermy was acquired twice among synapsids, by the non-*Dicynodon* Dicynodontoidea and the Eucynodontia. The optimization of our results onto the

phylogeny using the parsimony method suggests a different pattern (Fig. 4): endothermy was acquired only once among synapsids, by the last common ancestor of Neotherapsida (i.e. the last common ancestor of mammals and *Oudenodon* more than 260 My ago). Once endothermy was acquired by the last common ancestor of Neotherapsida, taxa within this clade are expected to show high mass-independent resting metabolic rate values. Natural selection may have promoted slight variations in the mass-independent resting metabolic rate of *Oudenodon*, *Lystrosaurus* and *Moghreberia,* but the inferred values fall within the range of variation observed in extant mammals (Fig. 4).

In conclusion, quantitative histology and phylogenetic eigenvector maps developed by Guénard *et al.* (2013) and recently used by Legendre *et al.* (2016) allowed us to better constrain the temporal (more than 260 My ago) and phylogenetic (Neotherapsida) frames of the acquisition of mammalian endothermy.

ACKNOWLEDGEMENTS

We would like to express our gratitude to L. Legendre (Bloemfontein National Museum, South Africa) for helping us with statistical analyses, to A. de Ricqlès (Université Pierre et Marie Curie, Paris, France) and V. de Buffrénil (Muséum National d'Histoire Naturelle, Paris, France) for allowing access to collection specimens, and to H. Lamrous (UPMC) and S. Morel (MNHN) for the preparation of the thin sections. We also thank H. Bourget (MNHN) for the execution of the molds, L. Zylberberg (UPMC) for access to her

microscope. Many thanks also to Jennifer Botha-Brink, Kirstin Brink and an anonymous reviewer for their helpful comments.

REFERENCES

Botha J. 2003. Biological aspects of the Permian dicynodont *Oudenodon* (Therapsida, Dicynodontia), deduced from bone histology and cross-sectional geometry. *Palaeontologia Africana*. **39:** 37–44.

Botha J, Chinsamy A. 2000. Growth patterns deduced from the bone histology of the cynodonts *Diademodon* and *Cynognathus*. *Journal of Vertebrate Paleontology*. **20:** 705–711.

Botha J, Chinsamy A. 2004. Growth and life habits of the Triassic cynodont *Trirachodon*, inferred from bone histology. *Acta Palaeontologica Polonica*. **49:** 619–627.

Botha J, Chinsamy A. 2005. Growth patterns of *Thrinaxodon liorhinus*, a non-mammalian Cynodont from the Lower Triassic of South Africa. *Palaeontology*. **48:** 385–394.

Botha J, Smith RMH. 2007. *Lystrosaurus* species composition across the Permo-Triassic boundary in the Karoo Basin of South Africa: *Lystrosaurus* across the PTB. *Lethaia.* **40**: 125–137.

Botha-Brink J, Angielczyk KD. 2010. Do extraordinarily high growth rates in Permo-Triassic dicynodonts (Therapsida, Anomodontia) explain their success before and after the end-Permian extinction? *Zoological Journal of the Linnean Society*. **160:** 341–365.

Botha-Brink J, Abdala F, Chinsamy A. 2012. The radiation and osteohistology of nonmammaliaform cynodonts. In: Chinsamy-Turan A, ed. *Forerunners of Mammals: radiation, histology and biology.* Bloomington: Indiana Universiy Press, 223–246.

Burnham KP, Anderson DR, Huyvaert KP. 2011. AIC model selection and multimodel inference in behavioral ecology: some background, observations, and comparisons. *Behavioral Ecology and Sociobiology*. **65:** 3–35.

Castanet J, Croci S, Aujard F, Perret M, Cubo J, de Margerie E. 2004. Lines of arrested growth in bone and age estimation in a small primate: *Microcebus murinus*. *Journal of Zoology*. **263:** 31–39.

Chinsamy-Turan A. 2005. *The microstructure of dinosaur bone: deciphering biology with fine-scale techniques*. Baltimore: Johns Hopkins University Press.

Chinsamy A. 2012. The Microstructure of Bones and Teeth of Nonmammalian Therapsids. (2012). In: Chinsamy-Turan A, ed. *Forerunners of Mammals: radiation, histology and biology.* Bloomington: Indiana Universiy Press, 68–89.

Chinsamy A, Elzanowski A. 2001. Bone histology: evolution of growth pattern in birds. *Nature*. **412:** 402-403.

Chinsamy A, Hurum JH. 2006. Bone microstructure and growth patterns of early mammals. *Acta Palaeontologica Polonica*. **51:** 325–338.

Chinsamy A, Ray, S. 2012. Bone Histology of Some Therocephalians and Gorgonopsians, and Evidence of Bone Degradation by Fungi. In: Chinsamy-Turan A, ed. *Forerunners of Mammals: radiation, histology and biology.* Bloomington: Indiana Universiy Press, 199–221.

Chinsamy A, Rubidge BS. 1993. Dicynodont (Therapsida) bone histology: phylogenetic and physiological implications. *Palaeontologia Africana*. **30:** 97–102

Chinsamy A, Tumarkin-Deratzian A. 2009. Pathologic bone tissues in a Turkey Vulture and a nonavian dinosaur: Implications for interpreting endosteal bone and radial fibrolamellar bone in fossil dinosaurs. *Anatomical Record-Advances in Integrative Anatomy and Evolutionary Biology*. **292:** 1478–1484.

Cox CB. 1991. The Pangaea dicynodont *Rechnisaurus* and the comparative biostratigraphy of Triassic dicynodont faunas. *Palaeontology*. **34:** 767–784.

Cubo J, Le Roy N, Martinez-Maza C, Montes L. 2012. Paleohistological estimation of bone growth rate in extinct archosaurs. *Paleobiology*. **38:** 335–349.

Currey JD. 2003. The many adaptations of bone. *Journal of Biomechanics*. **36:** 1487–1495.

Dutuit JM. 1988. Ostéologie crânienne et ses enseignements, apports géologique et paléoécologique, de *Moghreberia nmachouensis*, Dicynodonte (Reptilia, Therapsida) du Trias supérieur marocain. *Bulletin du Muséum National d'Histoire Naturelle*. **3:** 227-285.

Florides GA, Kalogirou SA, Tassou SA, Wrobel L. 2001. Natural environment and thermal behaviour of *Dimetrodon limbatus*. *Journal of Thermal Biology*. **26:** 15–20.

Francillon-Vieillot H, de Buffrénil V, Castanet J, Géraudie J, Meunier FJ, Sire JY, Zylbeberg L, de Ricqlès A. 1990. Microstructure and mineralization of vertebrate skeletal tissues. In: Carter JG, ed. *Skeletal Biomineralization: Patterns, Processes and Evolutionary Trends*. New York: Van Nostrand Reinhold, 471–530.

Fröbisch J. 2007. The cranial anatomy of *Kombuisia frerensis* Hotton (Synapsida, Dicynodontia) and a new phylogeny of anomodont therapsids. *Zoological Journal of the Linnean Society*. **150:** 117–144.

Fröbisch J. 2009. Composition and similarity of global anomodont-bearing tetrapod faunas. *Earth-Science Reviews*. **95:** 119–157.

Gale TM. 1988. Comments on a “nest” of juvenile dicynodont reptiles. *Modern Geology*. **13:** 119–124.

Green J & Chinsamy-Turan A. 2012. Bone and dental histology of Late Triassic dicynodonts from North America. In: Chinsamy-Turan A, ed. *Forerunners of Mammals: radiation, histology and biology.* Bloomington: Indiana Universiy Press, 178–196.

Green JL, Schweitzer MH, Lamm ET. 2010. Limb bone histology and growth in *Placerias hesternus* (Therapsida: Anomodontia) from the Upper Triassic of North America. *Palaeontology*. **53:** 347–364.

Guenard G, Legendre P, Peres-Neto P. 2013. Phylogenetic eigenvector maps: a framework to model and predict species traits. *Methods in Ecology and Evolution*. **4:** 1120–1131.

Hacklander K, Arnold W & Ruf T. **2002**. Postnatal development and thermoregulation in the precocial European hare (*Lepus europaeus*). *Journal of Comparative Physiology B-Biochemical Systemic and Environmental Physiology* **172**: 183–190.

Houssaye A, Lindgren J, Pellegrini R, Lee AH, Germain D, Polcyn MJ. 2013. Microanatomical and histological features in the long bones of mosasaurine mosasaurs (Reptilia, Squamata) - Implications for aquatic adaptation and growth rates. *Plos One*. **8:** e76741.

Huttenlocker AK & Botha-Brink J. **2014**. Bone microstructure and the evolution of growth patterns in Permo-Triassic therocephalians (Amniota,Therapsida) of South Africa. *Peerj* **2**: e325.

Ji Q, Luo ZX, Yuan CX, Tabrum AR. 2006. A swimming mammaliaform from the Middle Jurassic and ecomorphological diversification of early mammals. *Science.* **311:** 1123–1127.

Kammerer CF, Fröbisch J, Angielczyk KD. 2013. On the validity and phylogenetic position of *Eubrachiosaurus browni*, a Kannemeyeriiform Dicynodont (Anomodontia) from Triassic North America. *PLoS ONE*. **8:** e64203.

Klein N. 2010. Long bone histology of Sauropterygia from the Lower Muschelkalk of the Germanic Basin provides unexpected implications for phylogeny. *PLoS ONE*. **5:** e11613.

Klein N. 2012. Postcranial morphology and growth of the pachypleurosaur *Anarosaurus heterodontus* (Sauropterygia) from the Lower Muschelkalk of Winterswijk, The Netherlands. *Paläontologische Zeitschrift*. **86:** 389–408.

Klein N, Sander PM, Krahl A, Scheyer TM, Houssaye A. 2016. Diverse Aquatic Adaptations in *Nothosaurus* spp. (Sauropterygia)—Inferences from Humeral Histology and Microanatomy. *PloS one*. **11:** e0158448.

Kolb C, Scheyer TM, Veitschegger K, Forasiepi AM, Amson E, Van der Geer AAE, Van den Hoek Ostend LW, Hayashi S, Sánchez-Villagra MR. 2015. Mammalian bone palaeohistology: a survey and new data with emphasis on island forms. *PeerJ*. **3:** e1358.

Konietzko-Meier D, Sander PM. 2013. Long bone histology of *Metoposaurus diagnosticus* (Temnospondyli) from the Late Triassic of Krasiejów (Poland) and its paleobiological implications. *Journal of Vertebrate Paleontology*. **33:** 1003–1018.

Konietzko-Meier D, Schmitt A. 2013. A histological study of a femur of *Plagiosuchus*, a Middle Triassic temnospondyl amphibian from southern Germany, using thin sections and micro-CT scanning. *Netherlands Journal of Geosciences*. **92:** 97–108.

Laurin M, de Buffrenil V. 2016. Microstructural features of the femur in early ophiacodontids: A reappraisal of ancestral habitat use and lifestyle of amniotes. *Comptes Rendus Palevol*. **15:** 115–127.

Lee AH. 2004. Histological organization and its relationship to function in the femur of *Alligator mississippiensis*. *Journal of Anatomy*. **204:** 197–207.

Legendre LJ, Segalen L, Cubo J. 2013. Evidence for high bone growth rate in *Euparkeria* obtained using a new paleohistological inference model for the humerus. *Journal of Vertebrate Paleontology*. **33:** 1343–1350.

Legendre LJ, Guénard G, Botha-Brink J, Cubo J. 2016. Paleohistological evidence for ancestral high metabolic rate in archosaurs. *Systematic Biology.* **65:** 989-996.

Maisch MW, Matzke AT. 2014. *Sungeodon kimkraemerae* n. gen. n. sp., the oldest kannemeyeriiform (Therapsida, Dicynodontia) and its implications for the early diversification of large herbivores after the P/T boundary. *Neues Jahrbuch für Geologie und Paläontologie*. **272:** 1-12.

Mauget C, Mauget R & Sempere A. 1999. Energy expenditure in European roe deer fawns during the suckling period and its relationship with maternal reproductive cost. *Canadian Journal of Zoology-Revue Canadienne De Zoologie* **77:** 389–396.

Meng QJ, Ji Q, Zhang YG, Liu D, Grossnickle DM, Luo ZX. 2015. An arboreal docodont from the Jurassic and mammaliaform ecological diversification. *Science*. **347:** 764-768.

Montes L, Le Roy N, Perret M, de Buffrenil V, Castanet J, Cubo J. 2007. Relationships between bone growth rate, body mass and resting metabolic rate in growing amniotes: a phylogenetic approach. *Biological Journal of the Linnean Society*. **92:** 63–76.

Montes L, Castanet J, Cubo J. **2010**. Relationship between bone growth rate and bone tissue organization in amniotes: first test of Amprino's rule in a phylogenetic context. *Animal Biology*. **60:** 25–41.

Padian K, de Ricqlès A, Horner JR. 2001. Dinosaurian growth rates and bird origins. *Nature*. **412:** 405–408.

Padian K, Horner JR, de Ricqlès A. 2004. Growth in small dinosaurs and pterosaurs: The evolution of archosaurian growth strategies. *Journal of Vertebrate Paleontology*. **24:** 555–571.

Padian K, Lamm ET. 2013. *Bone histology of fossil tetrapods: advancing methods, analysis, and interpretation*. Berkeley: University of California Press.

Padian K, Werning S & Horner JR. 2016. A hypothesis of differential secondary bone formation in dinosaurs. *Comptes Rendus Palevol* **15:** 40–48.

Ray S, Chinsamy A. 2004. *Diictodon feliceps* (Therapsida, Dicynodontia): bone histology, growth, and biomechanics. *Journal of Vertebrate Paleontology*. **24:** 180–194.

Ray S, Botha J, Chinsamy A. 2004. Bone histology and growth patterns of some nonmammalian therapsids. *Journal of Vertebrate Paleontology*. **24:** 634–648.

Ray S, Chinsamy A, Bandyopadhyay S. 2005. *Lystrosaurus murrayi* (therapsida, Dicynodontia): bone histology, growth and lifestyle adaptations. *Palaeontology*. **48:** 1169–1185.

Ray S, Bandyopadhyay S, Bhawal D. 2009. Growth patterns as deduced from bone microstructure of some selected neotherapsids with special emphasis on dicynodonts: Phylogenetic implications. *Palaeoword*. **18:** 53–66.

Ray S, Bandyopadhyay S, Appana R. 2010. Bone histology of a kannemeyeriid dicynodont *Wadiasaurus*: palaeobiological implications. In: Bandyopadhyay S, ed. *New aspects of mesozoic biodiversity.* Berlin: Springer Berlin Heidelberg, 73–89.

Ray S, Botha J, Chinsamy A. 2012. Dicynodont growth dynamics and lifestyle adaptations. In: Chinsamy-Turan A, ed. *Forerunners of Mammals: radiation, histology and biology.* Bloomington: Indiana Universiy Press, 121–148.

Reid REH. 1987. Bone and dinosaurian ‘‘endothermy’’. *Modern Geology*. **11:** 133–154.

Rey K. 2016. Thermophysiologie des thérapsides et changements climatiques du Permien et du Trias (300-200 Ma). PhD thesis.

Ricqlès Ad. 1969. Recherches paléohistologiques sur les os longs des Tétrapodes: Quelques observations sur la structure des os longs des Thériodontes. *Annales de Paléontologie.* **55:** 1–52.

Ricqlès Ad. 1972. Recherches paléohistologiques sur les os longs des Tétrapodes: Titanosuchiens, Dinocéphales et Dicynodontes. *Annales de Paléontologie.* **58:** 1–78.

Ricqlès Ad, Meunier FJ, Castanet J, Francillon-Vieillot H. 1991. Comparative microstructure of bone. *Bone*. **3:** 1-78.

Ricqlès Ad, Padian K, Horner JR. 2003. On the bone histology of some Triassic pseudosuchian archosaurs and related taxa. *Annales de Paléontologie*. **89:** 67–101.

Ricqlès Ad, Padian K, Knoll F, Horner JR. 2008. On the origin of high growth rates in archosaurs and their ancient relatives: Complementary histological studies on Triassic archosauriforms and the problem of a “phylogenetic signal” in bone histology. *Annales de Paléontologie*. **94:** 57–76.

Ruben J, Hillenius W, Kemp T, Quick D. 2012. The Evolution of Mammalian Endothermy. In: Chinsamy-Turan A, ed. *Forerunners of Mammals: radiation, histology and biology.* Bloomington: Indiana Universiy Press, 273–288.

Rubidge BS, Sidor CA. 2001. Evolutionary patterns among permo-triassic therapsids. *Annual Review of Ecology and Systematics*. **32:** 449–480.

Seltmann MW, Ruf T & Roedel HG. 2009. Effects of body mass and huddling on resting metabolic rates of post-weaned European rabbits under different simulated weather conditions. *Functional Ecology* **23:** 1070–1080.

Seymour RS, Bennett-Stamper CL, Johnston SD, Carrier DR, Grigg GC. 2004. Evidence for endothermic ancestors of crocodiles at the stem of archosaur evolution. *Physiological and Biochemical Zoology*. **77:** 1051–1067.

Seymour RS, Smith SL, White CR,Henderson DM, Schwarz-Wings D.. 2012. Blood flow to long bones indicates activity metabolism in mammals, reptiles and dinosaurs. *Proceedings of the Royal Society B-Biological Sciences*. **279:** 451–456.

Shelton C, Sander PM. 2015. *Ophiacodon* long bone histology: the earliest occurrence of FLB in the mammalia stem lineage. *PeerJ PrePrints*. **3:** e1262.

Shelton CD, Sander PM, Stein K, Winkelhorst H. 2013. Long bone histology indicates sympatric species of *Dimetrodon* (Lower Permian, Sphenacodontidae). *Earth and Environmental Science Transactions of the Royal Society of Edinburgh*. **103:** 217–236.

Skedros JG, Sorenson SM, Hunt KJ, Holyoak JD. 2007. Ontogenetic structural and material variations in ovine calcanei: A model for interpreting bone adaptation. *Anatomical Record-Advances in Integrative Anatomy and Evolutionary Biology*. **290:** 284–300.

Tumarkin-Deratzian AR. 2007. Fibrolamellar bone in wild adult *Alligator mississippiensis*. *Journal of Herpetology*. **41:** 341–345.

Smith R, Botha J. 2005. The recovery of terrestrial vertebrate diversity in the South African Karoo Basin after the end-Permian extinction. *Comptes Rendus Palevol*. **4:** 623–636.

Walter I, Seebacher F. 2009. Endothermy in birds: underlying molecular mechanisms. *Journal of Experimental Biology*. **212:** 2328–2336.

Woodward Ballard HN, Horner JR, Farlow JO. 2014. Quantification of intraskeletal histovariability in *Alligator mississippiensis* and implications for vertebrate osteohistology. *Peerj*. **2:** e422.

Zhou CF, Wu S, Martin T, Luo ZX. 2013. A Jurassic mammaliaform and the earliest mammalian evolutionary adaptations. *Nature*. **500:** 163–167.

FIGURE LEGENDS

Figure 1. *Moghreberia* nmachouensis (Triassic, Morocco): Mid-diaphyseal cross-section of stylopodial bones. (A) Humerus MNHN.F.ALM 297, (B) femur MNHN.F.ALM 100. Abbreviations: ant., anterior side; dor., dorsal side; lat., lateral side; med., medial side; post., posterior side; vent., ventral side. Scale bars represent 5 mm.

Figure 2. Qualitative histology of the *Moghreberia* humerus MNHN.F.ALM 297 (A-C) and femur MNHN.F.ALM 100 (D). (A) Secondary bone (remodelling with no formation of secondary osteons); arrow-heads point to cementing lines, (B) Secondary bone (Haversian remodelling) formed within a matrix of primary woven bone, (C) Alternation of zones (mainly made of woven bone) and annuli (made of parallel-fibered bone). The incipient FLB observed within zones contains a bone matrix formed of woven and parallel-fibered bone and sparse vascular canals, some of which form primary osteons. (D) Secondary osteons at the perimedullary zone. Abreviations: O1, primary osteon; O2, secondary osteon; PFB, parallel-fibered bone; WB, woven bone. Scale bars represent 0.1 mm.

Figure 3. Occurrence of FLB and/or incipient FLB in *Lystrosaurus* sp. (A-B) and *Oudenodon baini* (C). (A) Humerus 24.1: primary bone consisting of parallel-fibered bone and woven bone (incipient FLB). (B) Femur 11-15: FLB. (C) Unnumbered femur: FLB (also found in the humerus of this taxon). Scale bars represent 0.1 mm.

Figure 4. Mass-independent resting metabolic rate ($mLO_2\ h^{-1}\ g^{-0.67}$) for the species sampled in this study. For all extant taxa but *Lepus, Oryctolagus* and *Capreolus,* mass-independent resting metabolic rate (in $mLO_2\ h^{-1}\ g^{-0.67}$) f were experimentally quantified by Montes *et al.* (2007) and histological data are taken from Legendre *et al*. (2016). For *Lepus, Oryctolagus* and *Capreolus,* mass-independent resting metabolic rate were taken respectively from Hackländer *et al.* (2002), Seltmann *et al.* (2009) and Mauget *et al.* (1999) and histological data were quantified in this study. For extinct taxa, histological data were quantified in this study and mass-independent resting metabolic rate were estimated using phylogenetic eigenvector maps. For extant species red dots correspond to endotherms (mammals and birds) and blue dots to ectotherms (all other taxa). We show inferred values for the fossil taxa with the corresponding 95% confidence intervals. Arrow-head shows the acquisition of endothemy by synapsids.

Figure 1

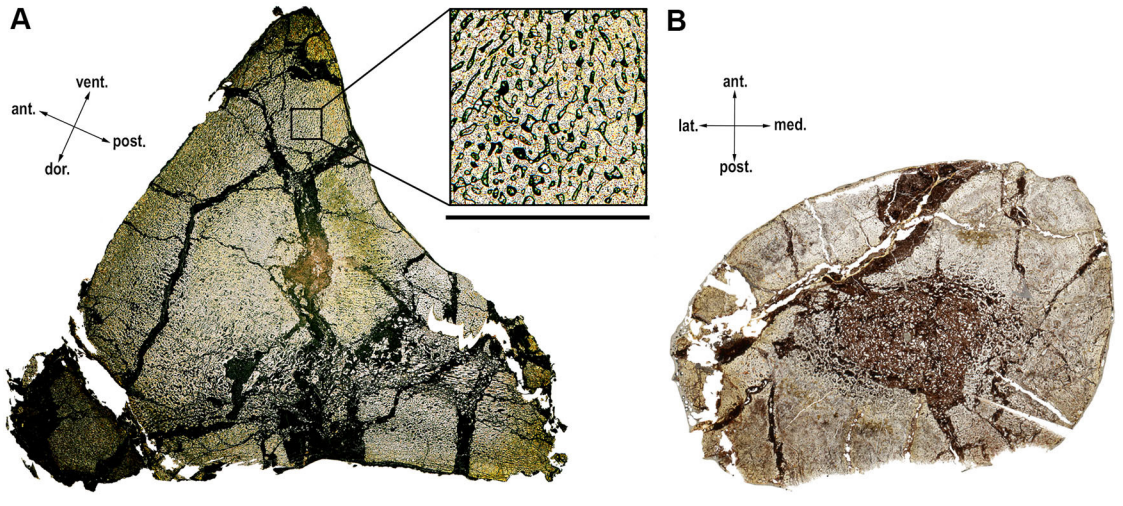

Figure 2

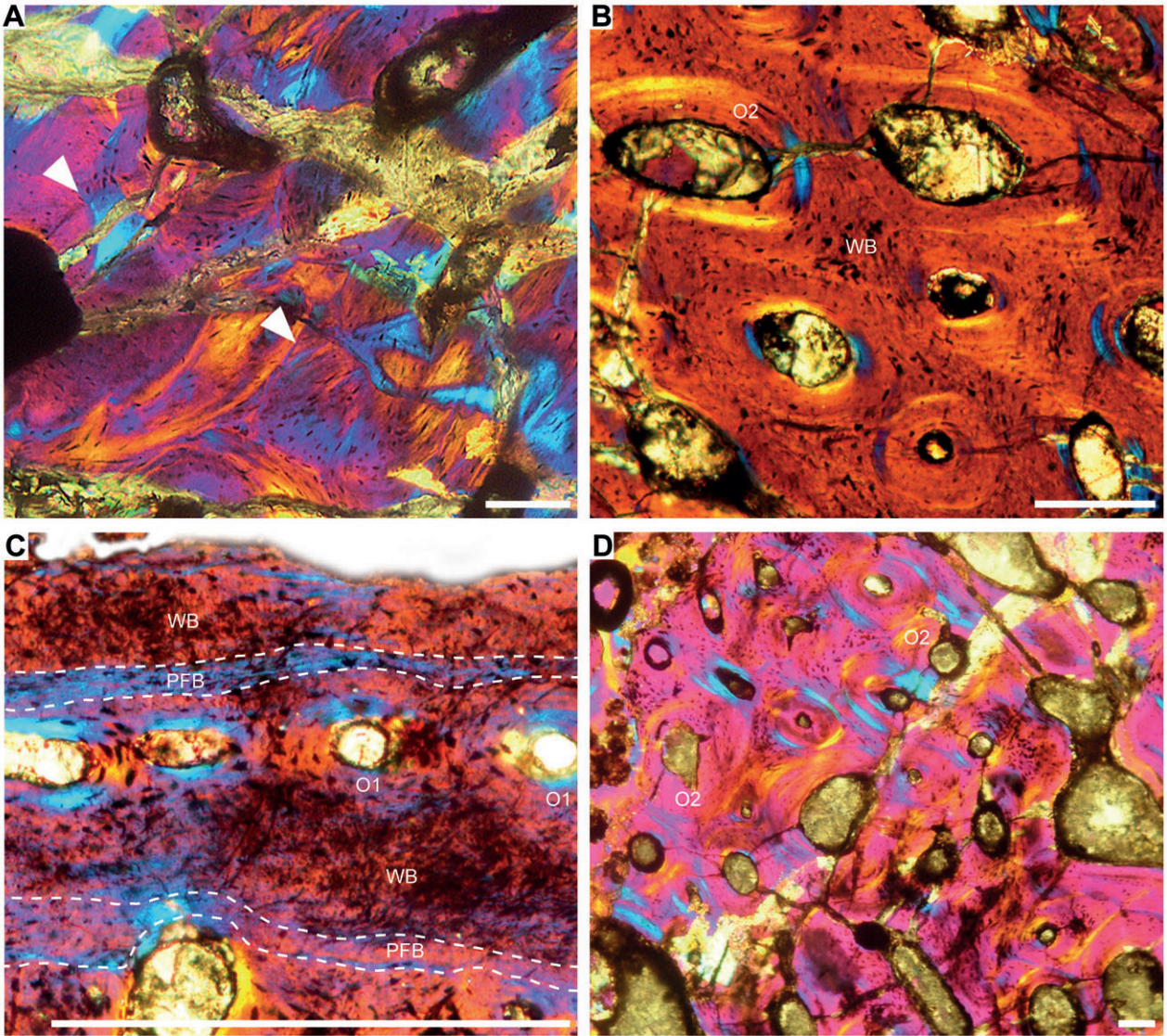

Figure 3

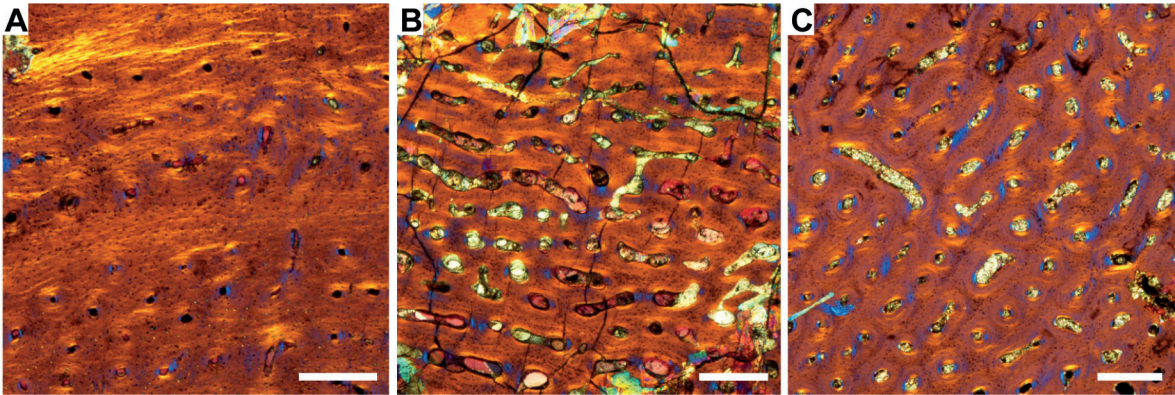

Figure 4

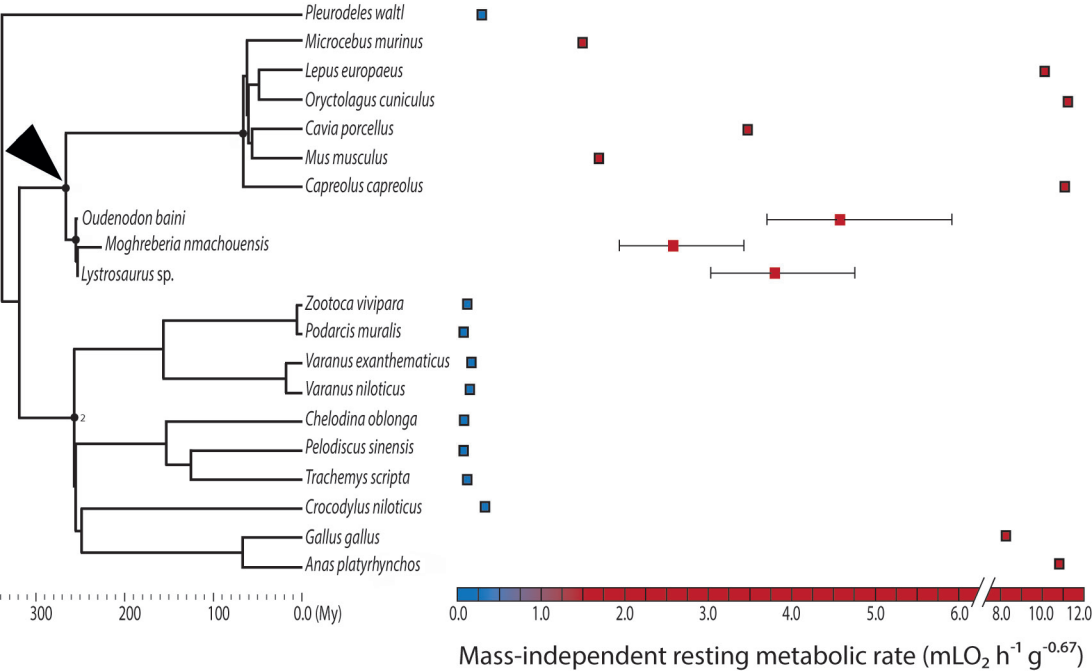
Pleurodeles waltl
Microcebus murinus
Lepus europaeus
Oryctolagus cuniculus
Cavia porcellus
Mus musculus
Capreolus capreolus
Oudenodon baini
Moghreberia nmachouensis
Lystrosaurus sp.
Zootoca vivipara
Podarcis muralis
Varanus exanthematicus
Varanus niloticus
2
Chelodina oblonga
Pelodiscus sinensis
Trachemys scripta
Crocodylus niloticus
Gallus gallus
Anas platyrhynchos
300
200
100
0.0 (My)
0.0
1.0
2.0
3.0
4.0
5.0
6.0
8.0
10.0
12.0
Mass-independent resting metabolic rate (mLO2 h-1 g-0.67)